EPHB2 knockdown mitigated MI-induced myocardial injury by inhibiting MAPK signaling

Hui Wang
Jinan Hospital
Ying Gao
Jinan Hospital
Deyun Liu
Jinan Hospital
Dong Xiao (DongXiao223@163.com)
Jinan Hospital

Research Article

Keywords: Myocardial infarction, EPHB2, MAPK pathway, Heart failure

Posted Date: November 2nd, 2021

DOI: https://doi.org/10.21203/rs.3.rs-1007249/v1

Abstract

Background

Myocardial infarction (MI) is a common disease in the cardiovascular field. The incidence of ventricular remodeling dysplasia and heart failure increases significantly after MI. The objective of this study was to investigate whether EPHB2 could regulate myocardial injury after MI and explore its regulatory pathways.

Methods

RT-qPCR and Western blot were used to verify the expression of EPHB2 in MI mice, and then shRNA knockdown of EPHB2 was used to confirm the relationship between EPHB2 expression and disease progression. The levels of inflammation, apoptosis and fibrosis were detected by tissue staining. Related factors were detected by RT-qPCR, Western blot or ELISA. Further, the signaling pathway through which EPHB affected MI processes was detected and preliminarily confirmed by Western blot.

Results

EPHB2 was significantly overexpressed in heart tissue of MI mice. Knockdown of EPHB2 gene significantly downregulated immune factors and apoptotic factors, and alleviated mi-induced cardiac tissue damage and functional decline in mice. The MAPK pathway was found to be a downstream pathway in which EPHB2 acted. Knockdown EPHB2 down-regulates phosphorylation of MAPK pathway-related proteins.

Conclusions

In mouse models, knockdown EPHB2 alleviated MI-induced cardiac function decline, inflammation and apoptosis of myocardial tissue, and myocardial fibrosis. This process may be achieved through the MAPK pathway.

Background

Myocardial infarction (MI) is a common cardiovascular disease with high morbidity and mortality. In recent years, with the popularization and application of vascularization therapy (such as percutaneous coronary intervention, coronary artery bypass grafting, etc.) and other treatment methods, the survival rate of acute myocardial infarction has been greatly improved. However, it also significantly increases the risk of ventricular remodeling, which significantly increases the incidence of heart failure [1, 2]. Among the factors involved in myocardial remodeling, myocardial fibrosis is the dominant factor. The imbalance of extracellular matrix synthesis and degradation is the main cause of myocardial fibrosis [3, 4]. In some cases, myocardial fibrosis is abnormally prolonged, resulting in abnormal heart function and hardening

of the ventricular wall, increasing the likelihood of heart failure [4, 5]. Therefore, it is very necessary to control the degree of myocardial fibrosis in a certain range.

The pathological basis of myocardial remodeling and impaired cardiac function after MI includes oxidative stress, inflammatory response, cytokine production, neuroendocrine changes, changes in hemodynamic load, etc. [6]. Inflammatory response in ischemic and reparative fibrosis plays an important role, the injury of myocardial cells release a lot of necrosis associated molecular patterns induced myocardial fibroblasts into proinflammatory phenotype, reactive oxygen species, IL-1 beta, and also induced myocardial fibroblasts secrete a large number of proinflammatory cytokines and chemokines, collect a large number of white blood cells, macrophages to myocardial locally. Subsequently, the inflammatory response was rapidly suppressed and the cell proliferation phase was transferred [7–9]. Oxidative stress occurs during ischemic injury, and the degree of oxidation exceeds the elimination of oxides, resulting in the imbalance between the oxidative system and the antioxidant system. Oxidative stress activates extracellular matrix metalloproteinase (MMPs) in myocardial fibroblasts by directly acting on cytokine and growth factor signal transduction. MMPs not only play a role in the degradation of cardiac matrix components, but also regulate the synthesis of collagen. The increased activity of MMPs increases the degree of myocardial fibrosis [10]. In addition, reactive oxygen species can also cause myocardial cell necrosis and apoptosis by activating a variety of signaling pathways, and can cause vascular endothelial dysfunction by inactivating carbon monoxide, further accelerating the development of myocardial fibrosis.

With the development of gene microarray and sequencing technology, comparing the transcriptome difference between pathological tissue and physiological tissue is beneficial to find the differentially expressed genes related to myocardial infarction. Immune-related pathways, cell cycle-related pathways, and extracellular matrix remodeling-related pathways were significantly increased after MI in mice. Several genes have also been identified to be associated with MI, such as Nppa, Serpina3n, and Anxa1, which are significantly altered after MI [11]. Recent studies have shown that 5-HTT Deficiency Affects Healing after Myocardial Infarction [12]. CTRP1 exacerbates cardiac dysfunction after myocardial infarction by regulating TLR4 in macrophages [13]. In the early stages of MI, TNFR2 agonist treatment improved left ventricular function. Regulation of TNFR1, on the other hand, has adverse effects [14]. Another research in monkeys, pigs, and rats showed that blocking the death checkpoint protein TRAIL improves cardiac function after MI [15].

Based on the above research background, we expected to screen the targets of tissue injury and fibrosis related proteins after myocardial infarction by bioinformatics methods and verify them in mouse MI model. Studies included detection of changes in the expression of related proteins at the protein level, detection of cardiac tissue apoptosis at the cellular level, assessment of pathological changes and fibrosis at the tissue level, and detection of blood flow at the overall level, prediction of the downstream pathway. Through the above experiments, we expect to find the key proteins of tissue damage and fibrosis after MI, so as to provide theoretical support for treating heart failure after MI with these proteins as targets.

Methods

Bioinformatics analysis

The expression profile datasets of patients with MI were searched from the publicly available Gene Expression Omnibus (GEO) database (http://www.ncbi.nlm.nih.gov/geo). In the GEO dataset (GSE141512), a transcriptome profiling in peripheral blood mononuclear cells of 6 MI patients and 6 healthy individuals was performed and the expression of EPHB2 was calculated.

CTD and String databases were used to screen out the signaling pathways through which EPHB2 affected MI. The pathways associated with myocardial infarction were screened from the CTD database. The pathways affected by EPHB2 are retrieved from the String database. The intersection of the two was taken to obtain the signaling pathway that mediated EPHB2's effect on MI, which was prepared for further verification.

Mice feeding and model establishment

C57BL/6J mice were purchased from Charles River Co., Ltd, China. Mice were allowed unlimited access to food and water throughout the study. The circadian was twelve hours in the light (7:00 am~ 7:00 pm) and the rest of twelve hours in the dark. The ambient temperature was 22±2°C. Relative humidity was 55±5%.

To knockdown EPHB2 specifically, AAV9-shEPHB2 was injected into mice via the jugular vein. The detailed procedure is as follows. Mice were anaesthetized with 1% isoflurane in oxygen, while viral solution (3×10^{11} vector genomes (vg)/mouse) was slowly injected via the jugular vein. MI model was established 4 weeks after administration.

To establish MI mouse model, left anterior descending (LAD) coronary occlusion was performed. As described above [16], The mice were anaesthetized by intraperitoneal injection of 1% phenobarbital sodium (30 mg/kg). After thoracotomy at the fourth intercostal space, the left thoracic cavity was exposed. The LAD coronary artery was ligated with a 6-0 suture at the lower edge of the left atrial appendage. The success of establishing the MI model was confirmed if there was an immediate color change on the heart surface after LAD ligation. Sham animals underwent the same surgical procedures, except the LAD was not occluded. Follow-up tests were conducted 4 weeks after the model was established.

RT-qPCR

Total RNA was extracted using Trizol reagent. then reverse transcribed into DNA using a RT-PCR Kit (Thermo #K1622), according to the manufacturer's instructions. Real-time PCR was performed with SYBR Green PCR kit (Thermo F-415XL) on a Real-Time PCR System (ABI-7500, USA) with GAPDH gene being used as internal control [17]. The $2^{-\Delta\Delta Ct}$ method was used to analyze the data [18]. The primers for qPCR

were purchased from Sangon Biotech Company (Shanghai, China) .primers were designed through Primer-BLAST tool [19]. Each sample was tested in triplicate.

The sequences of the primers for EPHB2:

Forward primer, TGGTCGTCATTGCCATCGTA,

Reverse primer, TTCATGCCTGGGGTCATGTG.

The sequences of the primers for CTGF:

Forward primer, AGAACTGTGTACGGAGCGTG,

Reverse primer, GTGCACCATCTTTGGCAGTG.

The sequences of the primers for Collagen I:

Forward primer, CGATGGATTCCCGTTCGAGT,

Reverse primer, CGATCTCGTTGGATCCCTGG.

The sequences of the primers for Collagen III:

Forward primer, TGACTGTCCCACGTAAGCAC,

Reverse primer, GAGGGCCATAGCTGAACTGA.

The sequences of the primers for GADPH:

Forward primer, GGGTCCCAGCTTAGGTTCAT,

Reverse primer, CCCAATACGGCCAAATCCGT.

Western blot assay

Western blot assay was used to detect protein expression levels. Proteins were extracted using RIPA total protein lysate (cat. no. P0013C, Beyotime, Inc, China) following the manufacturer's instructions. Proteins from each sample were separated by electrophoresis on 10% SDS-PAGE gels and transferred onto PVDF membranes (cat. no. FFP39, Beyotime, Inc, China). After incubation with blocking solution (cat. no. P0252, Beyotime, Inc, China), the PVDF membranes were separately incubated with anti EPHB2 antibody, anti Bax antibody, anti cleaved-caspase 3 antibody, anti Bcl-2 antibody, anti p-ERK antibody, anti ERK antibody, anti p-JNK antibody, anti JNK antibody, anti p-p38 antibody, anti p38 antibody and anti GAPDH antibody (cat.no. ab252935, ab32503, ab32042, ab182858, ab201015, ab184699, ab124956, ab179461, ab195049, ab31828 and ab8245, Abcam, Inc, USA,1:2000) at 4 °C overnight. After the blots were washed,

they were incubated with HRP-conjugated Goat Anti-Rabbit IgG H&L secondary antibody(cat.no. ab6721, Abcam, Inc, USA,1:2000) for 1.5 h and detected by ECL like Western reagent (cat. no. P0018S, Beyotime, Inc, China) with a chemiluminescent imaging system (ChemiDoc MP, Bio-Rad, Inc, USA).

Immunohistochemistry

EPHB2 expression was detected followed standard immunohistochemical protocol as reported elsewhere [20]. Briefly, paraffin-embedded slides (5 μM) were baked at 60°C, then dewaxed by xylene and rehydrated by fractionated ethanol. Antigen was extracted, and incubated with 3% H_2O_2 for 10 min. Then the slides were sealed with bovine serum for 1 h, and then anti EPHB2 antibody (cat. no. ab252935, Abcam, USA; 1:100 dilutions in 1% bovine serum albumin) were added and incubated at room temperature for 3 hours. The slides were covered with the secondary antibody and placed in a humid chamber for 1 hour, and then DAB was added to reveal the staining intensity. Sections were photographed using an Olympus IX81 microscope (Olympus, Inc, Japan).

Echocardiographic examination

Cardiac physiological analysis of mice was performed as previously described [21,22]. In brief, mice were anesthetized with i.p. injection of 1% phenobarbital sodium (30 mg/kg). A sector scanner (Sonos 1500; Hewlett-Packard) equipped with a 12-MHz transducer was used to record two-dimensionally guided M-mode tracings to assess left ventricle wall thickness, left ventricle dimensions, and fractional shortening. Electrocardiogram recordings were acquired on anesthetized mice with a multichannel amplifier and were converted to digital signals for analysis (PowerLab system; ADInstruments).

Hemodynamic measurements

Cardiac hemodynamic measurements were performed as described[23]. Mice were anesthetized with i.p. injection of 1% phenobarbital sodium (30 mg/kg), and the right common carotid artery was isolated and cannulated with a 1.4-F micromanometer (Millar Instruments). Maximal values of the instantaneous first derivative of LV pressure (+dp/dt max, as a measure of cardiac contractility) and minimum values of the instantaneous first derivative of LV pressure (−dp/dt min, as a measure of cardiac relaxation) were recorded.

The target pathway of Embelin was predicted by network pharmacology analysis

To predict the signaling pathways that embelin acts on, three networked pharmacological databases were used for analysis. Embelin was retrieved from CTD Database (Comparative Toxicgenomics Database, http://ctdbase.org/), STITCH Database (http://stitch.embl.de/) and BATMAN-TCM Database (Bioinformatics Analysis Tool for Molecular mechanism of Traditional Chinese Medicine, http://bionet.ncpsb.org.cn/batman-tcm/) to obtain the corresponding signaling pathways. Subsequently, "Kidney Cancer" was retrieved from the CTD Database and the corresponding signal

pathway was obtained. Winn diagram was used to analyze the results of four retrievals and the intersection was selected as the most likely target pathway of embelin.

Enzyme-linked immunosorbent assay (ELISA)

Blood samples were collected by extracting the eyeball. The whole blood was kept for 30 min and centrifuged at 2,000 × g for 20 min at room temperature, and the serum components were stored as aliquots at −80°C until further use. Lactate Dehydrogenase (LDH), Creatine Kinas(CK), TNF-α, IL-6, and IL-1β levels were measured using ELISA kits (cat.no. E-EL-M0419c, E-EL-M0358c, E-MSEL-M0002, E-EL-M0044c, and E-MSEL-M0003, Elabscience. Inc, China) according to manufacturer's instructions. Optical density values were measured with a microplate reader (Multiskan FC, Thermo scientific) in each well.

Histological stain

HE staining was performed with a Hematoxylin-Eosin/HE Staining Kit (cat. no. G1120, Solarbio, Inc, China) according to the manufacturer’s instructions. In brief, after dewaxing, slices were incubated with haematoxylin for 2 min and thereafter stained with eosin.

TUNEL staining was performed using a TUNEL Apoptosis Assay Kit (cat.no. C1088, Beyotime, Inc, China). Myocardial sections of mice were obtained and blocked for 1 h at room temperature in TBS containing 0.5% Triton X-100, 0.1% Na-Citrate, and 5% normal goat serum. Sections were washed in PBS twice for 5 min and incubated with the TUNEL labeling solution for 1 h at 37°C. Sections were then washed with PBS for 10 min at room temperature and Images were captured.

Masson Trichrome staining was used to detect fibrosis with a Masson's Trichrome Stain Kit(cat.no.G1340, Solarbio, Inc, China). Briefly, alcohol (100% alcohol, 95% alcohol 70% alcohol) was used to de-paraffinize and rehydrate cardiac tissue. To improve staining quality, Bouin's solution was applied for 15 minutes at 56°C and rinse under tap water for 5-10. Next, immerged in Weigert's iron hematoxylin solution 10 minutes then wash with PBS buffer 5 minutes. Afterward, stained with Biebrich scarlet-acid fuchsin solution for 5 minutes, then washed in distilled water. Then sections underwent series of differentiation, dehydration in 75% and 90% alcoho and rinsing in tap water. and cleared in xylene and mounted.

Images were captured by an Olympus IX81 microscope (Olympus, Inc, Japan) in bright-field mode.

Statistical analysis

The GraphPad Prism software (version 8.0) was used to perform Statistical analysis and mapping. One-way analysis of variance followed by a Bonferroni post-hoc test was used to analyze differences between groups. Data were considered significantly different when $p < 0.05$. Image analysis was conducted using ImageJ software (1.53c).

Results

##EPBH2 was significantly up-regulated after MI

To detect genes that might be involved in MI processes, we used the GEO database for screening. The dataset GSE141512 is used. Compared with healthy patients, EPBH2 transcription level was significantly increased in the tissues of MI patients, as shown in Figure1A. This result was replicated in the mouse MI model. As shown in Figure1B, qPCR results showed that compared with sham group, the transcription level of cardiac EPHB2 gene in MI group was significantly up-regulated. At the protein expression level, the expression of EPHB2 protein in mice in MI group was significantly enhanced, as shown in Figure 1C. The immunohistochemical results were consistent with the results of qPCR and western blot. As shown in Figure1D, the expression of EPHB2 was enhanced in the heart tissue of MI model mice.

##The downregulation of EPBH2 significantly alleviated the cardiac function damage after MI

To further examine the role of EPBH2 in the MI process, we injected AVV9-shEPHB2 jugular with the expectation of downregulating EPHB2 expression. As shown in Figure2A-B, compared with MI+ AAV 9-shNC group, the transcription level and protein expression level of cardiac EPHB2 in MI+AAV9-shEPHB2 group were significantly down-regulated. Heart function was then measured. As shown in Figure2C-E, echocardiography showed that the EF (left ventricular ejection fraction) and FS (left ventricular shortening fraction), were significantly decreased in mice after MI, and left ventricular systolic function was reduced and cardiac function was impaired. The hemodynamics results (dp/dt max and dp/dt min) showed the same trend (Figure2F-G). In addition, serum LDH and CK levels in MI model mice were significantly increased, as shown in Figure2H-I, which also indicated that heart function was impaired in MI model mice[24, 25]. In comparison with the MI+AVV9-shNC group, the heart function of the MI+AVV9-shEPHB2 group was significantly improved after the expression of EPHB2 was down-regulated by shEPHB2 (Figure 2C-I).

EPBH2 knockdown significantly alleviated the inflammation and apoptosis of heart tissue after MI

We then examined MI-induced inflammation and apoptosis in mouse heart tissue. As shown in Figure 3A, HE staining results showed that the infiltration level of inflammatory cells in the myocardial tissue of mice increased and edema appeared after the establishment of MI model. The inflammation level was reduced after down-regulation of EPHB2. ELISA results showed that the expression levels of inflammatory factors such as TNF-α, IL-6 and IL-1β in serum of mice were significantly up-regulated after the establishment of MI model, while the levels of inflammatory factors were also decreased after the down-regulation of EPHB2 (Figure 3B-D).

Similarly, after the establishment of MI model, a large number of myocardial cells in mice were apoptotic, and western blot results also showed that the expression of apoptotic factors was enhanced. The

expression of apoptotic factors in the MI+AAV-shNC group was down-regulated compared with that in the MI+AAV-shNC group (Figure4A-E).

Knockdown of EPBH2 significantly alleviated MI-induced myocardial fibrosis

Cardiac fibrosis is the main cause of heart failure after MI[4]. Masson Trichrome Staining was used to detect the level of myocardial fibrosis in mice. As shown in Figure 5A, the level of myocardial fibrosis in mice was significantly increased after the establishment of MI model, and decreased after the down-regulation of EPHB2 level. The change trend of transcription level of related factors detected by qPCR was consistent with the results of tissue staining (Figure 5B)

EPBH2 may act through the MAPK pathway

These results indicated that MI induced the up-regulation of EPHB2 expression in the myocarum of mice. Down-regulation of EPHB2 reversed MI-induced cardiac function decline, myocardial tissue inflammation and apoptosis, and myocardial fibrosis. The signaling pathway EPHB2 is involved in is unclear. We used the CTD database to retrieve MI-related pathways and interacted with the EPHB2-related pathways retrieved from the String database, and five signaling pathways were detected (Figure 6A). Western blot analysis showed that the phosphorylation levels of MAPK signaling pathway related proteins such as ERK, JNK, p38 were significantly up-regulated after MI, while the phosphorylation levels were partially restored after down-regulation of EPHB2 (Figure 6B-E).

Discussion

This study confirms that EPHB2 is involved in cardiac function decline after MI. The expression of EPHB2 was up-regulated by MI. Down-regulation of EPHB2 alleviated MI-induced cardiac function decline, myocardial tissue inflammation and apoptosis, and myocardial fibrosis. EPHB2 was predicted to act through the MAKP pathway by bioinformatics analysis and was validated by Western blot analysis. In conclusion, EPHB2 promotes cardiac function decline after MI through MAKP pathway.

Eph receptors are cell surface molecules that have a wide range of biological functions and affect a variety of cellular behaviors [26, 27]. There are 10 EphA receptors, and 6 EphB receptors [28]. Previous studies have found that Eph receptors are involved in ischemia-reperfusion injury. In both in-vivo and in-vitro mouse model of renal ischemia-reperfusion injury, EphA2 was up-regulated through an Src kinase–dependent pathway [29]. The expression levels of EphB4 and EphA2 were up-regulated in hypoxic skin, suggesting that Eph receptor was involved in revascularization after hypoxic injury [30]. EPHB2 is an important member of the Eph receptor family and has previously been shown to be expressed mainly in endothelial and tumor cells [31, 32]. More recently, EPHB2 has been found to also be expressed on a number of immune cells, including T cells, monocytes, and macrophages [33, 34]. Furthermore, EphB2 specifically binds to ephrin B1/B2 and activates forward signaling that promotes T cell migration and

monocyte activation [34, 35]. EphrinB2/EPHB2 promoted synaptic germination and synaptic strengthening in the colonic plexus via the ERK-MAPK pathway in a PI-IBS rat study [36].

MAPK pathway is involved in the regulation of various biological cell processes and becomes active due to various stress responses. It plays an important role in the proliferation and differentiation of stem cells and the regulation of related differentiation genes. Evidence for the involvement of the MAPK pathway in cardiovascular disease has been presented in patients with Noonan syndrome. As a genetic disease, it is mainly caused by multiple gene mutations in the MAPK pathway [37]. 80% of patients with Noonan syndrome have a congenital heart defect [38, 39]. These findings based on genetic diseases also suggest that the MAPK pathway is closely related to heart function and development. Another study found that ANP and BNP maintain myocardial cGMP levels to regulate cardiomyocyte p38 MAPK activity, sensitizing the heart to stress induced ventricular arrhythmias [40]. Recent studies have shown that KLF15 overexpression can reduce cardiomyocyte apoptosis and improve cardiac dysfunction in MI mice partly by inhibiting the p38 /MAPK signaling pathway [41].

In conclusion, silencing EPHB2 mitigated MI-induced cardiac function decline, myocardial tissue inflammation and apoptosis, and myocardial fibrosis in mouse models. This process may be achieved through the MAPK pathway.

Declarations

Ethics approval and consent to participate

The experimental protocol of our study was performed in accordance with the Guide for the Care and Use of Laboratory Animals and approved by Jinan Hospital.

Consent for publication

None.

Availability of data and material

The datasets used and/or analysed during the current study are available from the corresponding author on reasonable request.

Competing interests

The authors declare that they have no conflicts of interest.

Funding

None.

Authors' contributions

Conception and design: H W; Perform experiment: H W and Y G; Data analysis and technical support: DY L and D X; Manuscript writing: H W.

All authors have read and approved the manuscript

Acknowledgements

None.

References

1. Braunwald E (2015) The war against heart failure: the Lancet lecture. Lancet 385 (9970):812–824
2. Bui AL, Horwich TB, Fonarow GC (2011) Epidemiology and risk profile of heart failure. Nat Rev Cardiol 8 (1):30–41
3. Kong P, Christia P, Frangogiannis NG (2014) The pathogenesis of cardiac fibrosis. Cell Mol Life Sci 71 (4):549–574
4. van den Borne SW, Diez J, Blankesteijn WM, Verjans J, Hofstra L, Narula J (2010) Myocardial remodeling after infarction: the role of myofibroblasts. Nat Rev Cardiol 7 (1):30–37
5. Fan Z, Guan J (2016) Antifibrotic therapies to control cardiac fibrosis. Biomater Res 20:13
6. Teufel A, Becker D, Weber SN, Dooley S, Breitkopf-Heinlein K, Maass T, Hochrath K, Krupp M, Marquardt JU, Kolb M, Korn B, Niehrs C, Zimmermann T, Godoy P, Galle PR, Lammert F (2012) Identification of RARRES1 as a core regulator in liver fibrosis. J Mol Med (Berl) 90 (12):1439–1447
7. Torre-Amione G, Kapadia S, Lee J, Durand JB, Bies RD, Young JB, Mann DL (1996) Tumor necrosis factor-alpha and tumor necrosis factor receptors in the failing human heart. Circulation 93 (4):704–711
8. Francis SE, Holden H, Holt CM, Duff GW (1998) Interleukin-1 in myocardium and coronary arteries of patients with dilated cardiomyopathy. J Mol Cell Cardiol 30 (2):215–223
9. Plenz G, Song ZF, Reichenberg S, Tjan TD, Robenek H, Deng MC (1998) Left-ventricular expression of interleukin-6 messenger-RNA higher in idiopathic dilated than in ischemic cardiomyopathy. Thorac Cardiovasc Surg 46 (4):213–216
10. Siwik DA, Pagano PJ, Colucci WS (2001) Oxidative stress regulates collagen synthesis and matrix metalloproteinase activity in cardiac fibroblasts. Am J Physiol Cell Physiol 280 (1):C53-60
11. Li D, Zhang J, Li J (2019) Role of miRNA Sponges in Hepatocellular Carcinoma. Clin Chim Acta
12. Popp S, Schmitt-Bohrer A, Langer S, Hofmann U, Hommers L, Schuh K, Frantz S, Lesch KP, Frey A (2021) 5-HTT Deficiency in Male Mice Affects Healing and Behavior after Myocardial Infarction. J Clin Med 10 (14)
13. Gu Y, Hu X, Ge PB, Chen Y, Wu S, Zhang XW (2021) CTRP1 Aggravates Cardiac Dysfunction Post Myocardial Infarction by Modulating TLR4 in Macrophages. Front Immunol 12:635267

14. Gouweleeuw L, Wajant H, Maier O, Eisel ULM, Blankesteijn WM, Schoemaker RG (2021) Effects of selective TNFR1 inhibition or TNFR2 stimulation, compared to non-selective TNF inhibition, on (neuro)inflammation and behavior after myocardial infarction in male mice. Brain Behav Immun 93:156–171
15. Wang Y, Zhang H, Wang Z, Wei Y, Wang M, Liu M, Wang X, Jiang Y, Shi G, Zhao D, Yang Z, Ren Z, Li J, Zhang Z, Wang Z, Zhang B, Zong B, Lou X, Liu C, Wang Z, Zhang H, Tao N, Li X, Zhang X, Guo Y, Ye Y, Qi Y, Li H, Wang M, Guo R, Cheng G, Li S, Zhang J, Liu G, Chai L, Lou Q, Li X, Cui X, Gao E, Dong Z, Hu Y, Chen YH, Ma Y (2020) Blocking the death checkpoint protein TRAIL improves cardiac function after myocardial infarction in monkeys, pigs, and rats. Sci Transl Med 12 (540)
16. Zhai C, Qian G, Wu H, Pan H, Xie S, Sun Z, Shao P, Tang G, Hu H, Zhang S (2020) Knockdown of circ_0060745 alleviates acute myocardial infarction by suppressing NF-kappaB activation. J Cell Mol Med 24 (21):12401–12410
17. Okazaki K, Sakamoto K, Kikuchi R, Saito A, Togashi E, Kuginuki Y, Matsumoto S, Hirai M (2007) Mapping and characterization of FLC homologs and QTL analysis of flowering time in Brassica oleracea. Theor Appl Genet 114 (4):595–608
18. Livak KJ, Schmittgen TD (2001) Analysis of relative gene expression data using real-time quantitative PCR and the 2(-Delta Delta C(T)) Method. Methods 25 (4):402–408
19. Ye J, Coulouris G, Zaretskaya I, Cutcutache I, Rozen S, Madden TL (2012) Primer-BLAST: a tool to design target-specific primers for polymerase chain reaction. BMC Bioinformatics 13:134
20. Pagliari M, Munari F, Toffoletto M, Lonardi S, Chemello F, Codolo G, Millino C, Della Bella C, Pacchioni B, Vermi W, Fassan M, de Bernard M, Cagnin S (2017) Helicobacter pylori Affects the Antigen Presentation Activity of Macrophages Modulating the Expression of the Immune Receptor CD300E through miR-4270. Front Immunol 8:1288
21. McMullen JR, Shioi T, Zhang L, Tarnavski O, Sherwood MC, Kang PM, Izumo S (2003) Phosphoinositide 3-kinase(p110alpha) plays a critical role for the induction of physiological, but not pathological, cardiac hypertrophy. Proc Natl Acad Sci U S A 100 (21):12355–12360
22. Shioi T, Kang PM, Douglas PS, Hampe J, Yballe CM, Lawitts J, Cantley LC, Izumo S (2000) The conserved phosphoinositide 3-kinase pathway determines heart size in mice. EMBO J 19 (11):2537–2548
23. Krishnamurthy P, Rajasingh J, Lambers E, Qin G, Losordo DW, Kishore R (2009) IL-10 inhibits inflammation and attenuates left ventricular remodeling after myocardial infarction via activation of STAT3 and suppression of HuR. Circ Res 104 (2):e9-18
24. Fan H, Yang L, Fu F, Xu H, Meng Q, Zhu H, Teng L, Yang M, Zhang L, Zhang Z, Liu K (2012) Cardioprotective effects of salvianolic Acid a on myocardial ischemia-reperfusion injury in vivo and in vitro. Evid Based Complement Alternat Med 2012:508938
25. Yin XL, Shen H, Zhang W, Yang Y (2011) Inhibition of endoplasm reticulum stress by anisodamine protects against myocardial injury after cardiac arrest and resuscitation in rats. Am J Chin Med 39 (5):853–866

26. Diegelmann RF, Evans MC (2004) Wound healing: an overview of acute, fibrotic and delayed healing. Front Biosci 9:283–289
27. Martin P, Parkhurst SM (2004) Parallels between tissue repair and embryo morphogenesis. Development 131 (13):3021–3034
28. Unified nomenclature for Eph family receptors and their ligands, the ephrins. Eph Nomenclature Committee (1997). Cell 90 (3):403–404
29. Baldwin C, Chen ZW, Bedirian A, Yokota N, Nasr SH, Rabb H, Lemay S (2006) Upregulation of EphA2 during in vivo and in vitro renal ischemia-reperfusion injury: role of Src kinases. Am J Physiol Renal Physiol 291 (5):F960-971
30. Vihanto MM, Plock J, Erni D, Frey BM, Frey FJ, Huynh-Do U (2005) Hypoxia up-regulates expression of Eph receptors and ephrins in mouse skin. FASEB J 19 (12):1689–1691
31. Salvucci O, de la Luz Sierra M, Martina JA, McCormick PJ, Tosato G (2006) EphB2 and EphB4 receptors forward signaling promotes SDF-1-induced endothelial cell chemotaxis and branching remodeling. Blood 108 (9):2914–2922
32. Wang SD, Rath P, Lal B, Richard JP, Li Y, Goodwin CR, Laterra J, Xia S (2012) EphB2 receptor controls proliferation/migration dichotomy of glioblastoma by interacting with focal adhesion kinase. Oncogene 31 (50):5132–5143
33. Stimamiglio MA, Jimenez E, Silva-Barbosa SD, Alfaro D, Garcia-Ceca JJ, Munoz JJ, Cejalvo T, Savino W, Zapata A (2010) EphB2-mediated interactions are essential for proper migration of T cell progenitors during fetal thymus colonization. J Leukoc Biol 88 (3):483–494
34. Braun J, Hoffmann SC, Feldner A, Ludwig T, Henning R, Hecker M, Korff T (2011) Endothelial cell ephrinB2-dependent activation of monocytes in arteriosclerosis. Arterioscler Thromb Vasc Biol 31 (2):297–305
35. Alfaro D, Munoz JJ, Garcia-Ceca J, Cejalvo T, Jimenez E, Zapata A (2008) Alterations in the thymocyte phenotype of EphB-deficient mice largely affect the double negative cell compartment. Immunology 125 (1):131–143
36. Zhang L, Wang R, Bai T, Xiang X, Qian W, Song J, Hou X (2019) EphrinB2/ephB2-mediated myenteric synaptic plasticity: mechanisms underlying the persistent muscle hypercontractility and pain in postinfectious IBS. FASEB J 33 (12):13644–13659
37. Johnston JJ, van der Smagt JJ, Rosenfeld JA, Pagnamenta AT, Alswaid A, Baker EH, Blair E, Borck G, Brinkmann J, Craigen W, Dung VC, Emrick L, Everman DB, van Gassen KL, Gulsuner S, Harr MH, Jain M, Kuechler A, Leppig KA, McDonald-McGinn DM, Can NTB, Peleg A, Roeder ER, Rogers RC, Sagi-Dain L, Sapp JC, Schaffer AA, Schanze D, Stewart H, Taylor JC, Verbeek NE, Walkiewicz MA, Zackai EH, Zweier C, Members of the Undiagnosed Diseases N, Zenker M, Lee B, Biesecker LG (2018) Autosomal recessive Noonan syndrome associated with biallelic LZTR1 variants. Genet Med 20 (10):1175-1185
38. Pierpont ME, Digilio MC (2018) Cardiovascular disease in Noonan syndrome. Curr Opin Pediatr 30 (5):601–608

39. Shaw AC, Kalidas K, Crosby AH, Jeffery S, Patton MA (2007) The natural history of Noonan syndrome: a long-term follow-up study. Arch Dis Child 92 (2):128–132
40. Hall EJ, Pal S, Glennon MS, Shridhar P, Satterfield SL, Weber B, Zhang Q, Salama G, Lal H, Becker JR (2021) Cardiac natriuretic peptide deficiency sensitizes the heart to stress induced ventricular arrhythmias via impaired CREB signaling. Cardiovasc Res
41. Wang B, Xu H, Kong J, Liu D, Qin WD, Bai W (2021) Kruppel-like factor 15 reduces ischemia-induced apoptosis involving regulation of p38/MAPK signaling. Hum Gene Ther

Figures

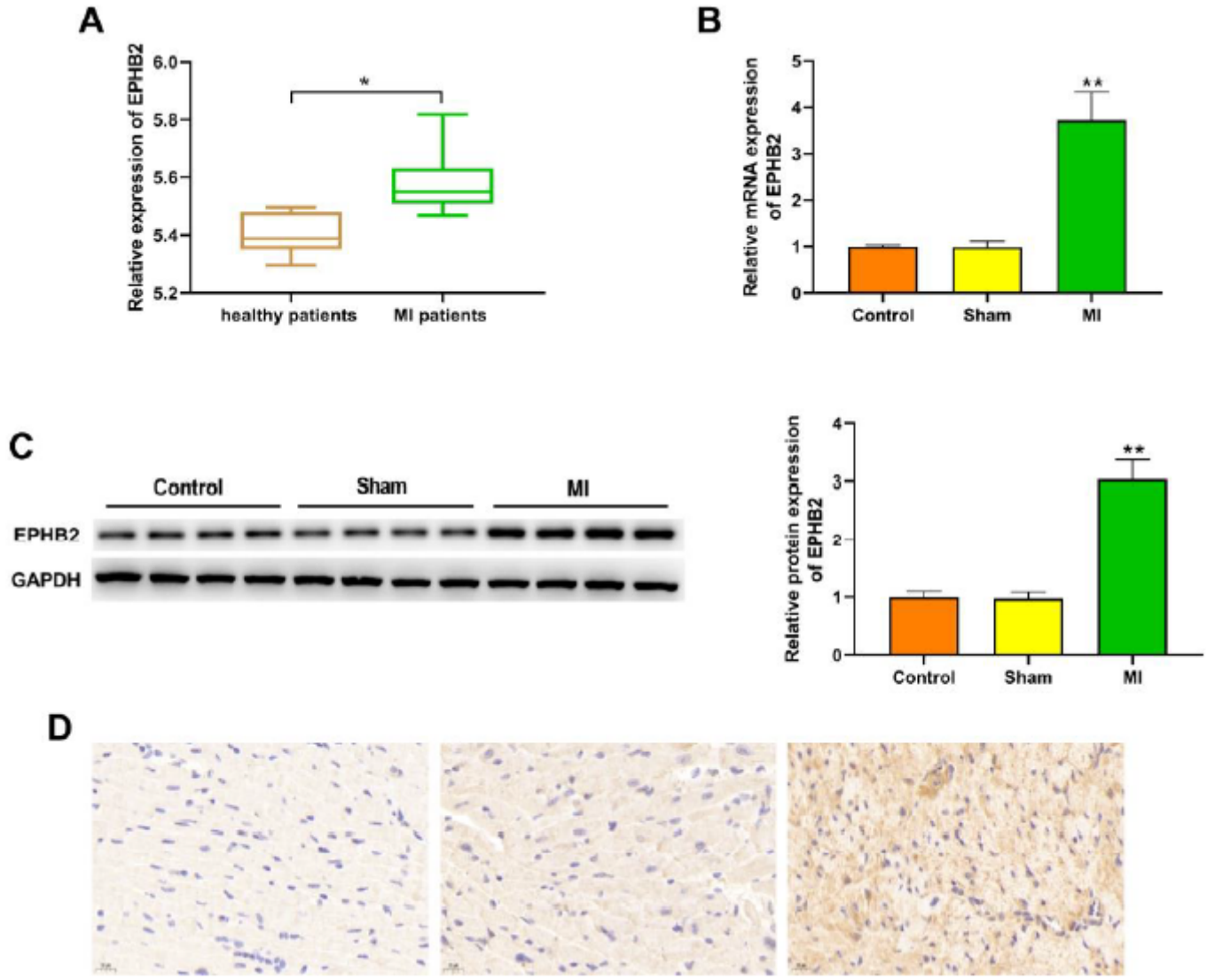

Figure 1

EPBH2 was significantly up-regulated after MI. (A) Analysis of GSE141512 microarray showed that EPHB2 was highly expressed in MI patients, *P<0.05 compared with healthy patients; (B) RT-qPCR

showed that the transcription level of EPHB2 in MI mice was significantly up-regulated compared with that in Sham group; (C) Western blot results showed that the expression level of EPHB2 in MI mice was significantly up-regulated compared with that in SHAM group; (D) Immunohistochemistry showed that EPHB2 expression was up-regulated in heart tissue of MI mice. **P<0.01 compared with sham group.

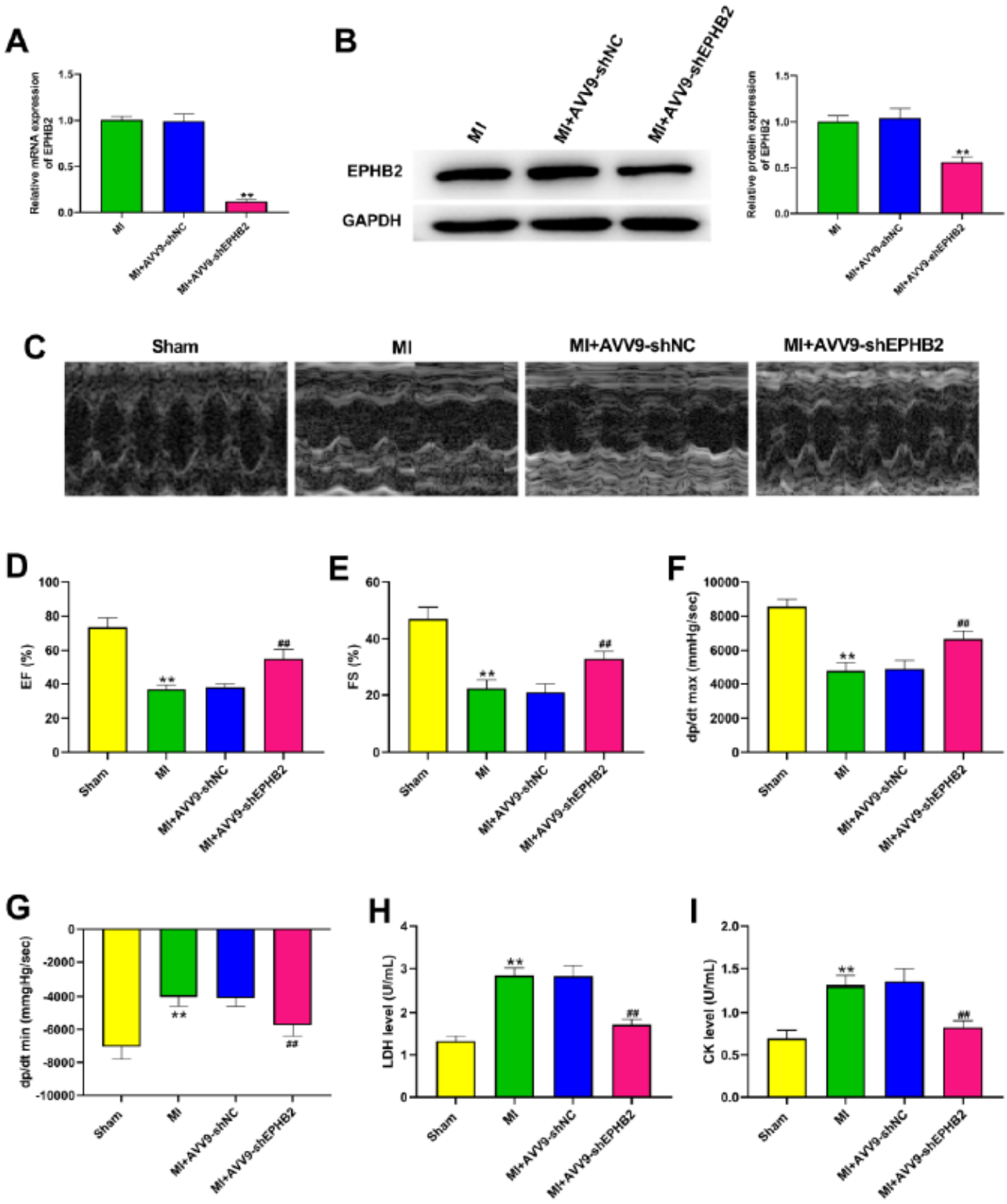

Figure 2

The downregulation of EPBH2 significantly alleviated the cardiac function damage after MI. (A) shEPHB2 significantly down-regulated the transcription level of EPHB2 in MI mice; (B) shEPHB2 significantly down-regulated the expression level of EPHB2 protein in MI mice; (C) Ultrasonic cardiogram of mice in each group; (D) Ejection fraction decreased significantly in MI group and partially recovered after EPHB2 knockdown; (E) The shortening fraction was significantly decreased in the MI group and partially recovered after knockdown of EPHB2; (F) The maximal dp/dt was significantly decreased in the MI group and partially recovered after knockdown of EPHB2; (G) The minimal dp/dt was significantly decreased in the MI group and partially recovered after knockdown of EPHB2; (H) Serum LDH in MI group increased and partially recovered after inhibiting EPHB2; (I) Serum CK in MI group increased and partially recovered after inhibiting EPHB2. (A-B) **P<0.01 compared with MI+AAV9-shNC group, (D-I) **P<0.01 compared with Sham group, ##P<0.01 compared with MI+AAV9-shNC group.

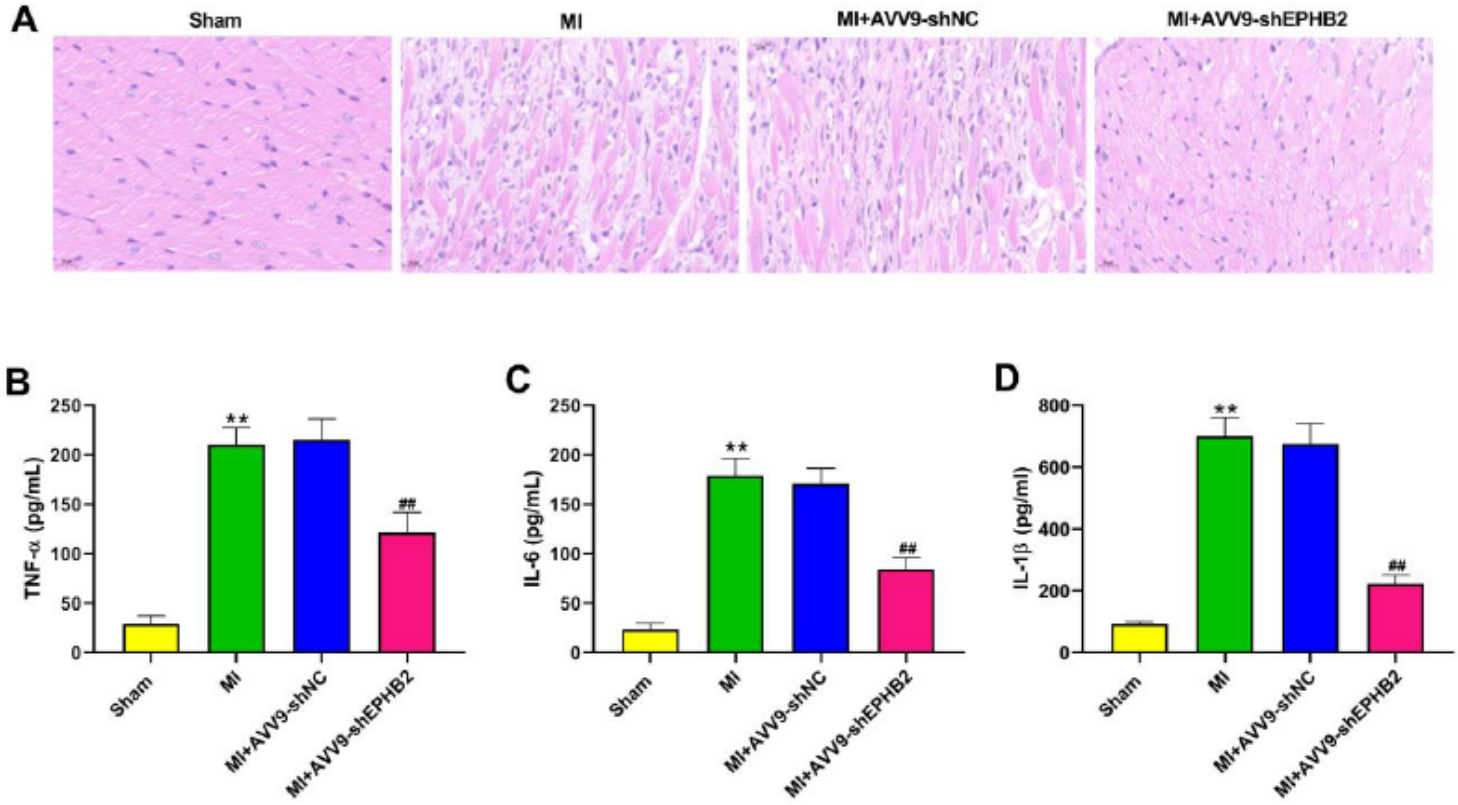

Figure 3

EPBH2 knockdown significantly alleviated the inflammation of heart tissue after MI. (A) HE staining showed that MI induced myocardial tissue inflammation, which was relieved after knockdown of EPHB2; (B) TNF-α was up-regulated in MI mice, and was relieved after knockdown of EPHB2; (C) IL-6 was up-regulated in MI mice, and was relieved after knockdown of EPHB2; (D) IL-1β was up-regulated in MI mice, and was relieved after knockdown of EPHB2. **P<0.01 compared with Sham group, ##P<0.01 compared with MI+AAV9-shNC group.

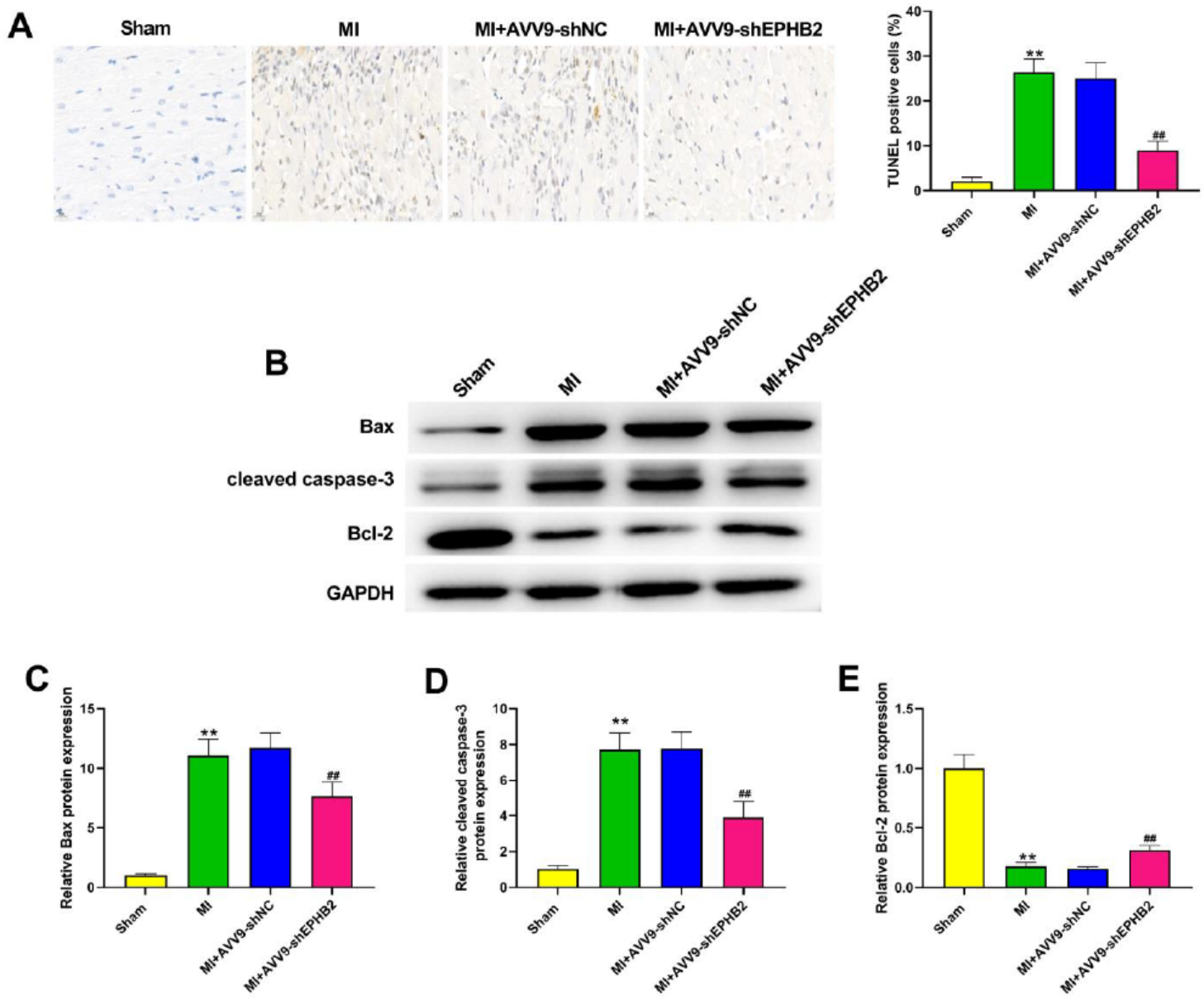

Figure 4

EPBH2 knockdown significantly alleviated apoptosis of heart tissue after MI. (A) TUNEL staining showed that MI induced autophagy, which was decreased after knockdown of EPHB2; (B) Western blot diagram of autophagy factors; (C) Bax expression level was up-regulated by MI, which was relieved after knockdown of EPHB2; (D) Cleaved caspase-3 expression level was up-regulated by MI, which was relieved after knockdown of EPHB2; (E) Bcl-2 expression level was down-regulated by MI, which was relieved after knockdown of EPHB2. **P<0.01 compared with Sham group, ##P<0.01 compared with MI+AAV9-shNC group.

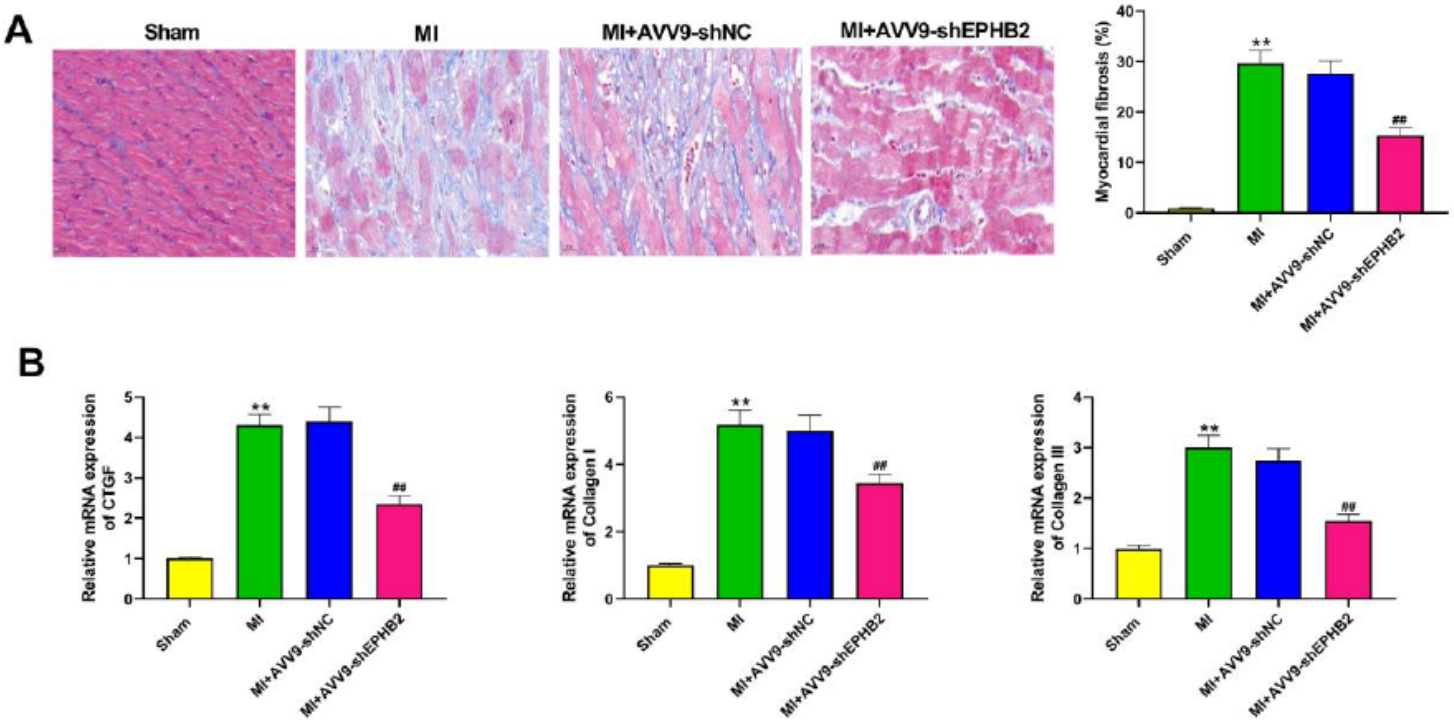

Figure 5

Knockdown of EPBH2 significantly alleviated MI-induced myocardial fibrosis. (A) Cardiac fibrosis induced by MI was alleviated after knockdown of EPHB2; (B) Rt-qpcr results showed that mi-induced up-regulation of fibrosis factor transcription was reversed after knockdown of EPHB2. **P<0.01 compared with Sham group, ##P<0.01 compared with MI+AAV9-shNC group.

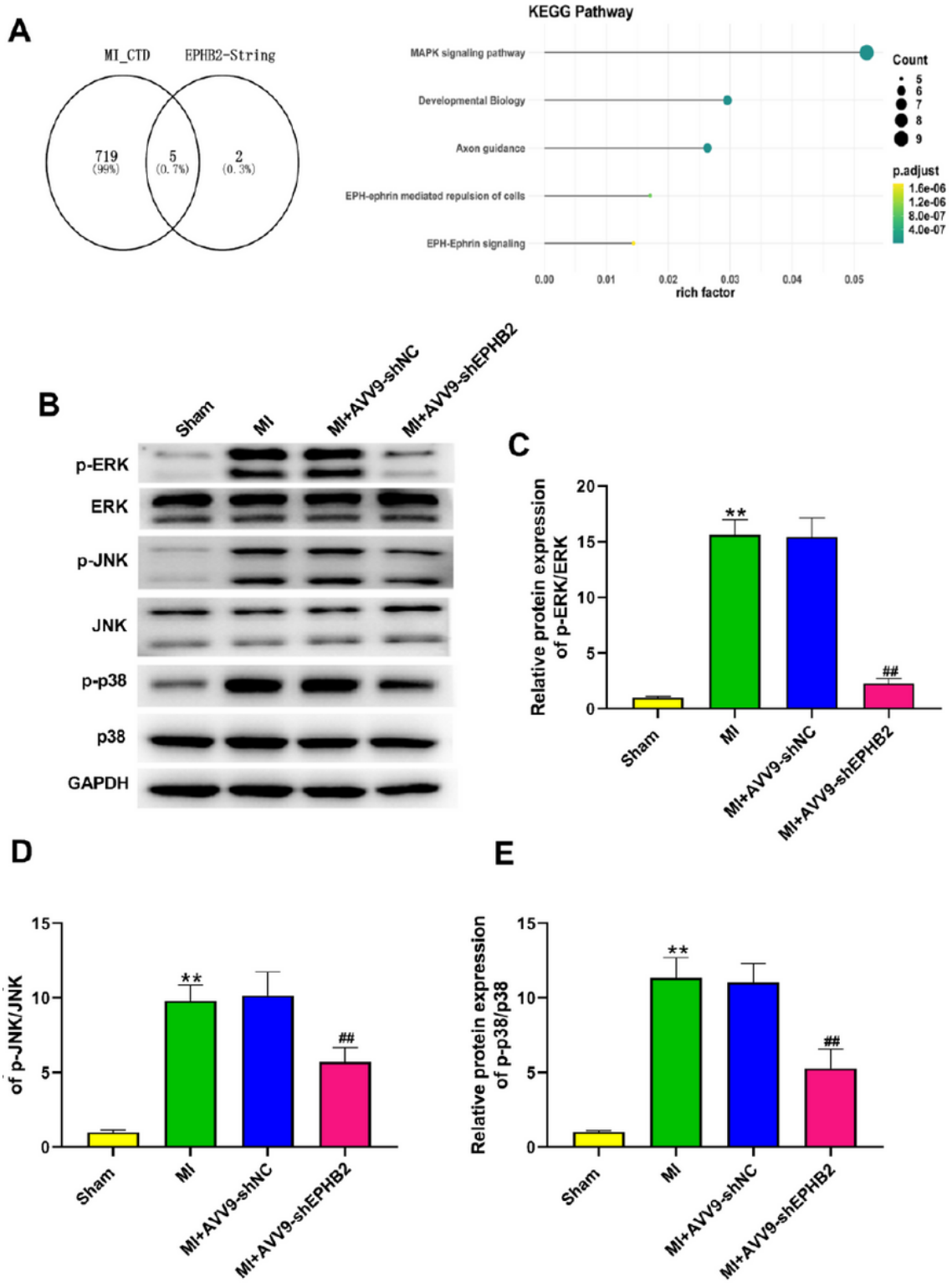

Figure 6

EPBH2 may act through the MAPK pathway. (A) Bioinformatics analysis indicated that EPHB2 might affect MI process through MAPK pathway; (B) Western blot diagram of proteins in MAPK pathway; (C) The phosphorylation of ERK protein was up-regulated by MI, and was alleviated after knockdown of EPHB2; (D) The phosphorylation of JNK protein was up-regulated by MI, and was alleviated after knockdown of EPHB2; (E) The phosphorylation of p38 protein was up-regulated by MI, and was alleviated

after knockdown of EPHB2. **P<0.01 compared with Sham group, ##P<0.01 compared with MI+AAV9-shNC group.